DISCHARGE PATTERNS
OF SWIMMERET MOTONEURONES IN THE LOBSTER,
SIMULATED WITH A DIGITAL COMPUTER

BY W. J. DAVIS* AND R. K. MURPHEY

Department of Biology, University of Oregon, Eugene, Oregon 97403

INTRODUCTION

A satisfactory understanding of the central nervous mechanisms underlying a particular behaviour requires information about the nature of the input to single participating motor nerve cells. In the case of swimmeret beating in lobsters, the participating motoneurones discharge in repetitive bursts which contain from one to several impulses each. In general, the intervals between successive spikes in each burst decrease during the first half of the burst, and increase during the last half. This finding led to the hypothesis that during swimmeret beating each participating motoneurone receives an excitatory input which varies with time in a sinusoidal fashion, at a frequency identical to that of swimmeret beating (Davis, 1969).

In the present paper the implications of this hypothesis are explored by experiments on a computer-simulated neurone. We have found that the response of the artificial neurone to a sinusoidal excitation reproduces the output of single swimmeret moto-neurones in all respects, including many which were unforeseen. Moreover, slight changes in the membrane parameters of the simulated neurone produce the full range of output exhibited by swimmeret motoneurones. The results of the simulation experiments therefore support the proposed hypothesis.

METHODS

The simulation was performed on an IBM/360 computer. Biological results were obtained by methods described in previous papers (Davis, 1968*a*, 1969).

Properties of the simulated neurone

The artificial neurone was simulated in accord with generally accepted properties of nerve cells (Fig. 1). Thus, the neurone was given a threshold for spike generation, an absolute and a relative refractory period. The initial spike of a burst was generated when the excitatory input (see below) first crossed the threshold value. Each spike was followed by an 8 msec. period of absolute refractoriness, during which the threshold value was effectively infinite. Following the absolute refractory period the threshold value decayed exponentially from an arbitrary value of 10 times the original threshold back to the initial threshold. The half-decay time of the threshold function was varied from 1 to 20 msec.

*Present address, Department of Biological Sciences, Stanford University, Stanford, California 94305.

Properties of the simulated excitatory input

The simulated excitatory input varied sinusoidally with time, with minima always occurring at zero (Fig. 1). Maxima were varied between 1 and 10 times the threshold value. The period of the oscillation was varied between 250 and 1000 msec. and was inversely proportional to the amplitude, in accord with constraints developed elsewhere (Davis, 1968b, 1969). The amount of time during which the excitatory input exceeded the threshold value during each burst was held constant during a given experiment, since the burst duration in swimmeret motoneurones is independent of the frequency of swimmeret beating (Davis, 1969).
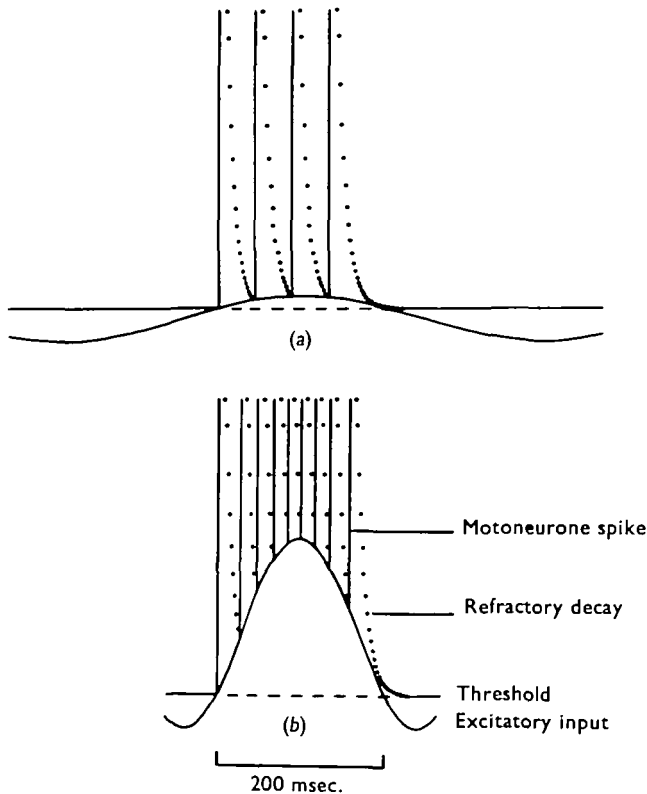

Fig. 1. Plots of the computer output during low-frequency (*a*) and high-frequency (*b*) sinusoidal excitation of the simulated neurone. Computations of the threshold and excitatory input values were performed every 2 msec.

RESULTS

Variation in the number of spikes per cycle

The function relating the period of the sinusoidal input to its amplitude is approximately hyperbolic. When the time above threshold is held constant at 200 msec., asymptotes occur at an input period of about 250 msec. and an amplitude equal to the threshold value (Fig. 2). Plots of the amplitude of the sinusoidal input wave against the number of spikes per cycle show that the relationship is approximately
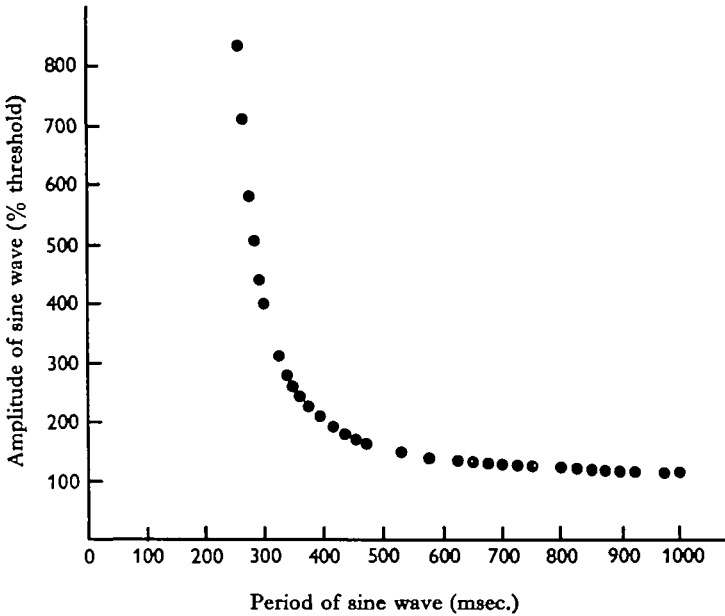
Fig. 2. Amplitude of the computer-generated sinusoidal excitatory wave plotted against its period. The amount of time per cycle during which the amplitude of the excitatory wave exceeded the threshold value was maintained at 200 msec. during the experiment.
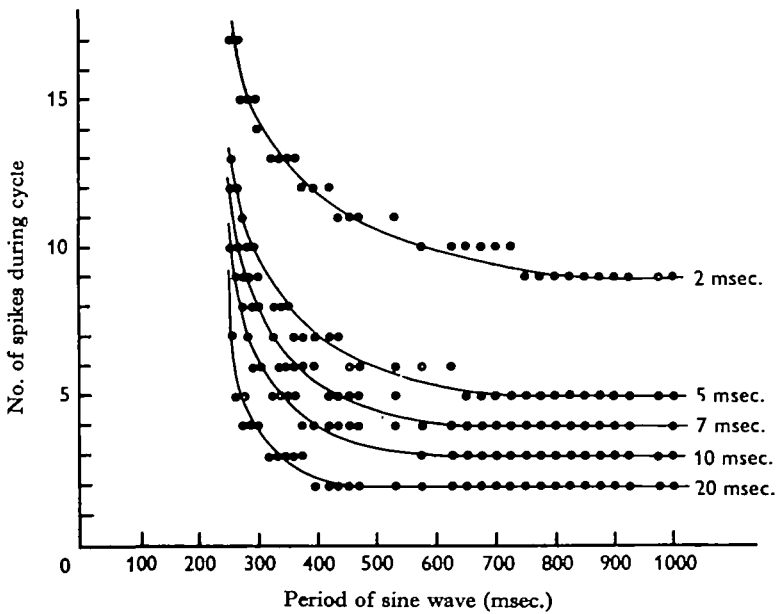

Fig. 3. Number of spikes per cycle produced by the simulated neurone plotted against the period of the sinusoidal excitatory input. The number to the right of each curve shows the duration of the half-decay time of the refractory recovery during the experiment. The time above threshold was held constant at 200 msec. during all experiments.

linear. Therefore, the relationship between the period of the sinusoidal input and the number of spikes per cycle is approximately hyperbolic (Fig. 3).

Variation in the half-decay time of the refractory recovery following each spike in the simulated neurone changes the shape and the position of the curve which relates the period of the sinusoidal input to the number of spikes per cycle. As the refractory decay time is increased, the curve is depressed and its average slope is increased (Fig. 3). The position of the curve is also altered by changing the amount of time per cycle during which the amplitude of the excitatory wave exceeds the value of
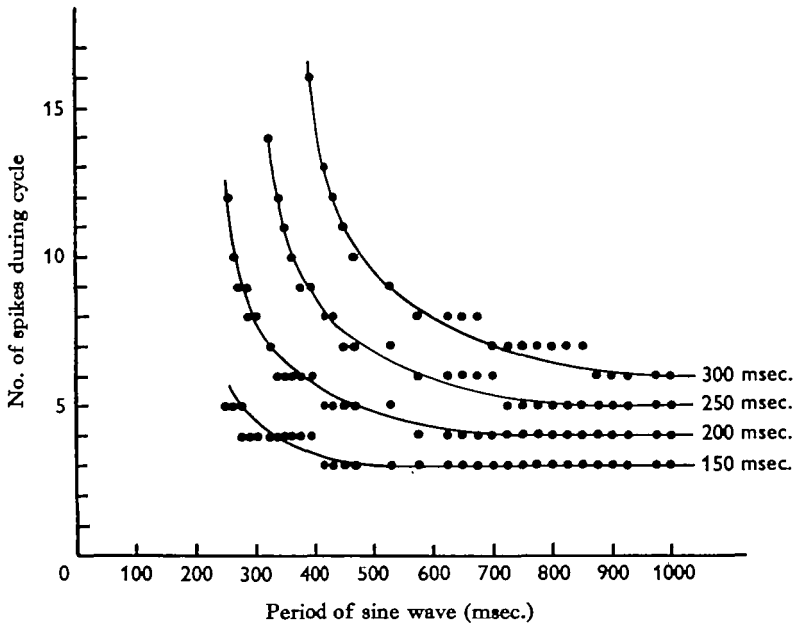

Fig. 4. Number of spikes per cycle produced by the simulated neurone plotted against the period of the sinusoidal excitatory input. The number to the right of each curve shows the amount of time per cycle during which the amplitude of the excitatory wave exceeded the threshold value. The duration of the half-decay time of the refractory recovery was held constant at 7 msec. during all experiments.

the threshold. The curve is depressed as the time above threshold is decreased, but the average slope of the curve is not affected (Fig. 4). Decreasing the time spent above threshold during each cycle is of course the mathematical equivalent of increasing the threshold value. Therefore, the different curves in Fig. 4 can be interpreted as the responses to the same excitatory inputs of simulated neurones having different thresholds for spike generation.

The behaviour of swimmeret motoneurones during swimmeret beating shows many parallels to the simulated output described above (Fig. 5). First, the relationship between the duration of the movement cycle and the number of spikes per cycle is approximately hyperbolic. Secondly, the minimum values of the two asymptotes are approximately the same as those of the simulated neurone. Thirdly, the curves for different swimmeret motoneurones occupy different positions and have different slopes, as would be expected for motoneurones heterogeneous with respect to refractory recovery time and with respect to threshold for spike generation.

Variation in the burst duration

The maintenance of the excitatory input wave above threshold for a constant amount of time during each cycle does not imply that the burst duration also remains constant. Instead, the burst duration varies in a 'sawtooth' fashion as the period of the sinusoidal input wave is increased, each 'tooth' corresponding to the loss of another spike from the burst (Fig. 6). The rising slope of each tooth decreases as the period of the sinusoidal input wave is increased. The range of the burst duration,
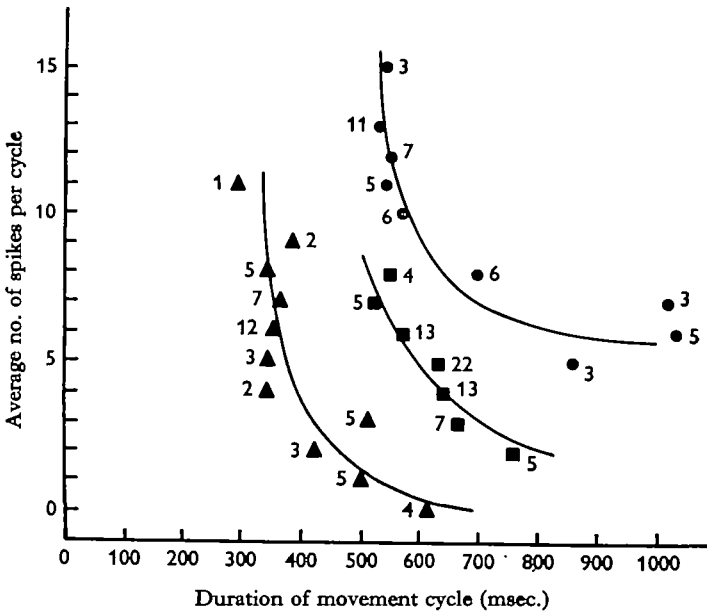
Fig. 5. Number of spikes per cycle produced by real swimmeret motoneurones plotted against the duration of the movement cycle. Each point is the average of the indicated number of bursts. ▲ and ■, activity of single motoneurones; ●, summed activity of three motoneurones innervating the same muscle.

i.e. the height of the tooth, is inversely proportional to the number of spikes per burst and therefore directly proportional to the duration of the refractory recovery period (Fig. 6).

Plots of the burst duration of real swimmeret motoneurones against the frequency of swimmeret beating have shown that there is no correlation between these two variables over the entire range of frequencies of swimmeret beating (Davis, 1969). Following the above simulation result, however, the biological data were re-examined and found to exhibit strong trends over limited ranges of frequencies of swimmeret beating (Fig. 7). The same sawtooth distribution as found in the output of the simulated neurone appears also in the output of the swimmeret motoneurones. As with the simulated output, the rising slope of each tooth decreases as the duration of the movement cycle increases, and the range of the burst duration is greater during movement cycles of long duration.
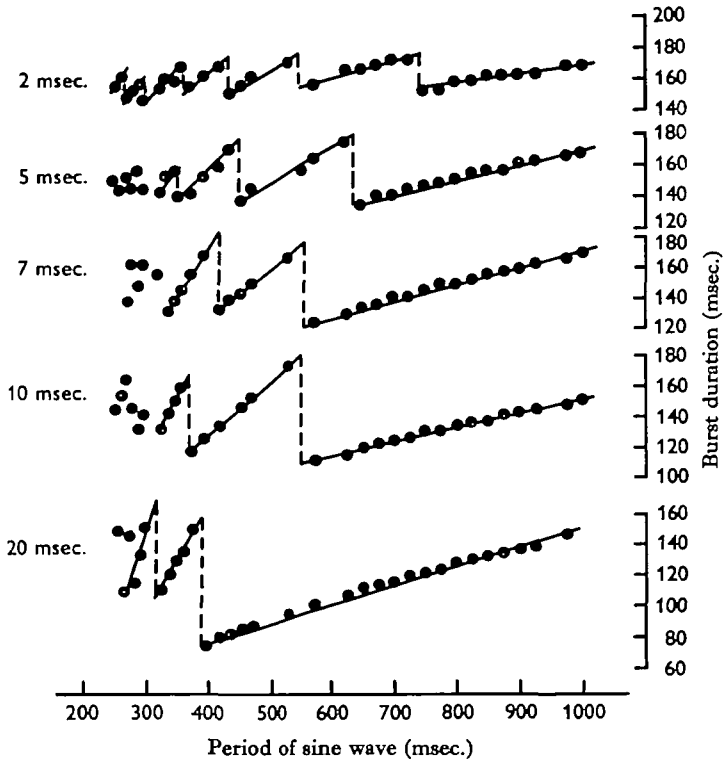
Fig. 6. Duration of bursts in the simulated neurone plotted against the period of the sinusoidal excitatory input. The number to the left of each curve shows the duration of the half-decay time of the refractory recovery during the experiment. The time above threshold was held constant at 200 msec. during all experiments.
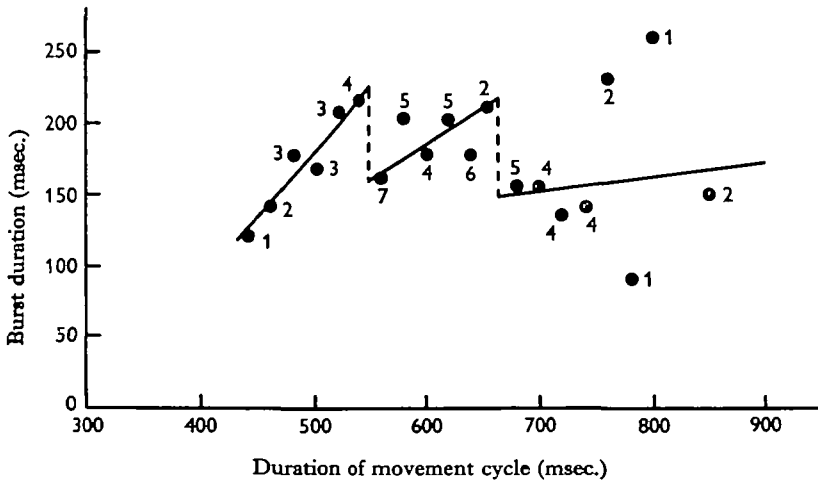

Fig. 7. Duration of bursts in real swimmeret motoneurones plotted against the duration of the movement cycle. Each point is the average of the number of bursts indicated.

Temporal structure of bursts

The temporal structure of the bursts of impulses within swimmeret motoneurones is described in the preceding paper (Davis, 1969, Fig. 17). The temporal structure of the bursts produced by the simulated neurone is similar. That is, the intervals between successive spikes in each burst decrease during the first half of the burst, and increase during the last half (Fig. 8). The range of the duration of the intervals within bursts increases as the duration of the refractory recovery period is increased (Fig. 8).
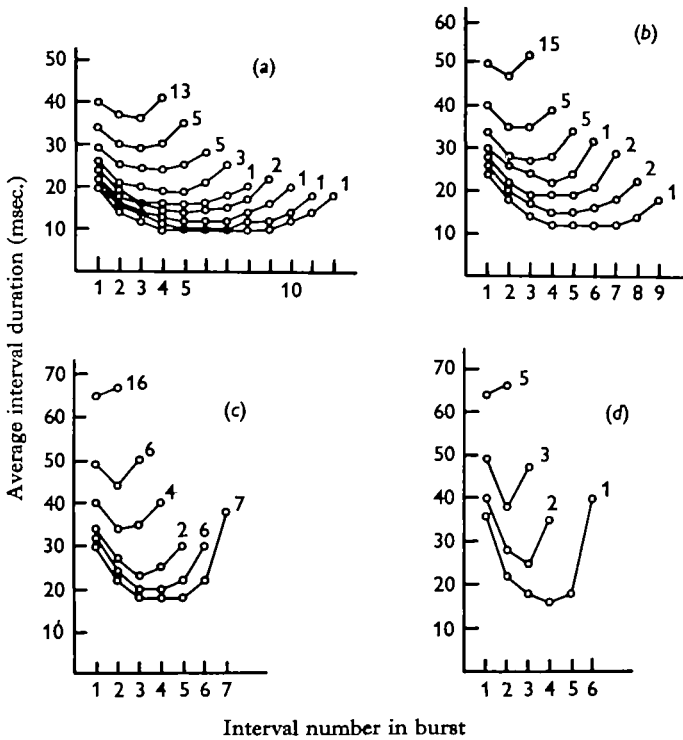

Fig. 8. Sequential histograms of the average interspike intervals within all bursts produced by the simulated neurone, for refractory half-decay times of (a) 5, (b) 7, (c) 10 and (d) 20 msec. Points representing a common burst size are connected to help to show the temporal structure of the bursts. Filled circles represent congruent points. The number to the right of each curve shows the number of bursts used to compute the curve.

The correspondence between the output of the unmodified simulated neurone and that of the swimmeret motoneurones is not exact on the extreme ranges of sinusoidal input frequencies. When only three spikes are contained within the burst of the simulated neurone, the last interval is the larger, but the difference between the two intervals is not as pronounced as in the bursts of the swimmeret motoneurones. This could mean that during low-frequency swimmeret beating the excitatory input to single motoneurones deviates from a sinusoidal waveform. When many spikes are contained within the burst of the simulated neurone, the last interval is usually the longest in the burst (Fig. 9), as in the bursts of the swimmeret motoneurones.
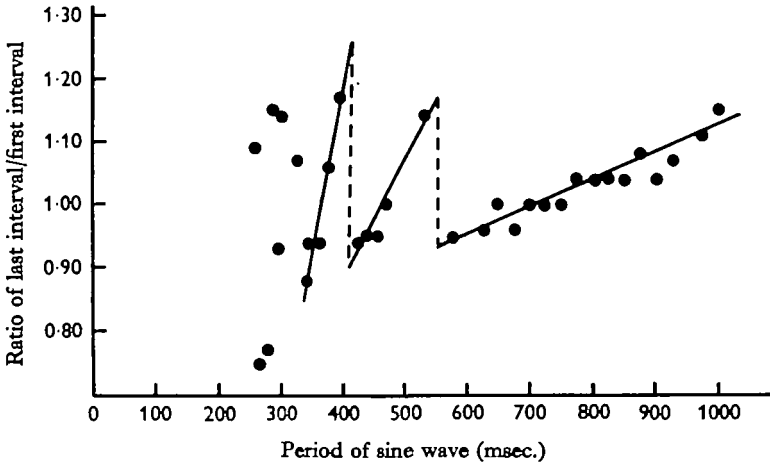
Fig. 9. The ratio of the last to the first interval in each burst of the simulated neurone, plotted against the period of the sinusoidal excitatory input. The half-decay time of the refractory recovery following each spike was 7 msec., while the time above threshold during each cycle was 200 msec.
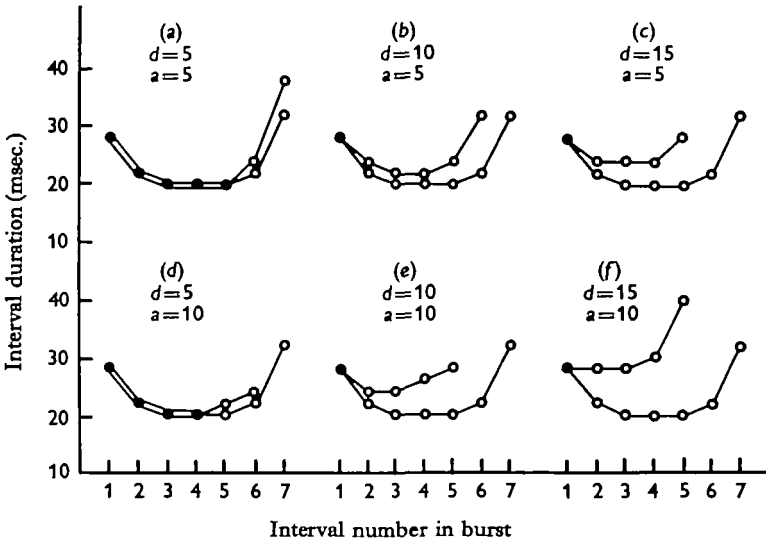

Fig. 10. Effect of accumulating refractoriness during each burst in the simulated neurone on the temporal structure of the burst. The amount of accumulating refractoriness increases from a to f. In each case the two curves show the sequential histograms of inter-spike intervals within a single simulated burst, before (lower curve in each case) and after (upper curve) adding a provision for accumulating refractoriness during the burst. Filled circles represent congruent points. In all cases the period of the sinusoidal excitatory input was 300 msec., the half-decay time of the refractory recovery was 7 msec., and the time above threshold was 200 msec. d, Half-time in msec. of the decay of the exponential curve relating the increment in refractoriness (delta) to the duration of the preceding inter-spike interval (see text), while a is the maximum value in msec. attained by delta, from which point the exponential decay was begun.

The preceding intervals are not constant in duration, however, as they are in the bursts of the swimmeret motoneurones.

We were unable to simulate the temporal structure of bursts containing many impulses by varying only the time course of the refractory recovery period following each spike. The desired output was obtained from the simulated neurone, however, by adding a provision for accumulating refractoriness during the course of each burst. This accumulation was achieved by increasing the half-decay time of the refractory recovery following each spike in the burst by a quantity, delta, whose value was inversely proportional to the duration of the immediately preceding interspike interval. The function relating delta to the duration of the preceding interval was exponential with a variable decay constant. As shown in Fig. 10, the presence of accumulating refractoriness 'flattens' the burst, i.e. reduces the range of the duration of the inter-spike intervals, and increases the relative duration of the intervals near the end of the burst.

<div align="center">DISCUSSION</div>

The close correspondence between the behaviour of the simulated neurone and that of the swimmeret motoneurones suggests that the respective excitatory inputs vary with time in the same way, i.e. sinusoidally. Some of the similarities between the simulated and real neurones must be interpreted with caution, however. For example, the sawtooth distribution of the burst duration (Fig. 6) is caused by holding the excitatory waveform above threshold for a fixed amount of time per cycle during frequency-correlated variation in the amplitude of the waveform, and does not depend upon the precise shape of the waveform. A sinusoidal waveform, however, provides the simplest explanation for the hyperbolic input–output curves (Figs. 2–5) and also for the temporal structure of individual bursts (Fig. 8). The position of the hyperbolic input–output curve of the simulated neurone (Fig. 2) provides a satisfactory teleology for the range of frequencies of swimmeret beating (1–4 cyc./sec.). In addition, the steepest portion of the curve, over which the 'control sensitivity' is the greatest, coincides with the most commonly encountered range of frequencies of swimmeret beating (2–3 cyc./sec.).

The excitatory input used in the present simulation was of course a continuous variable. The analogous input to the swimmeret motoneurones need not originate as a continuous function, however, since the integrative membrane of motoneurones behaves like a digital-to-analogue converter. Owing to this integrative capability the excitatory input to the swimmeret motoneurones could originate as a propagated wave of conventional action potentials in the ganglionic neuropile, as discussed in the preceding paper (Davis, 1969).

The rationale underlying the type of overt neural modelling described in the present paper is reviewed by Harmon & Lewis (1966). The present work reaffirms that such modelling can be useful to the biologist in at least three ways. First, it permits the rigorous formulation of a hypothesis and a rapid test of its feasibility. Secondly, it stimulates the re-examination of biological data, often resulting in new understanding and/or insight. Thirdly, overt modelling is a useful tool for planning further biological experimentation. The present work, for example, suggests that accumulating refractoriness during each burst of impulses in the swimmeret moto-

neurones of the lobster helps to determine the temporal structure of the burst, a hypo-
thesis which can be readily tested using biological preparations. Accumulating re-
fractoriness also plays a role in the production of the rhythmic motor discharge
patterns underlying locust flight (Wilson, 1964). The results of the present study
also encourage efforts to determine whether the ganglionic neuropile can support
a propagated wave of excitation having the required properties, and to record directly
this hypothetical central nervous activity.

SUMMARY

1. The response of a computer-simulated neurone to a sinusoidal excitatory
input was studied and compared to the rhythmic discharge patterns of swimmeret
motoneurones in the lobster.

2. All of the output parameters of the simulated neurone closely resemble those
of the swimmeret motoneurones, suggesting that the excitatory input to the swimmeret
motoneurones also varies with time in an approximately sinusoidal fashion.

3. The full range of behaviour exhibited by swimmeret motoneurones was obtained
from the simulated neurone by varying the time course of the refractory recovery
following each spike, the effective threshold for spike generation, and the rate of
accumulation of refractoriness during each burst.

REFERENCES

DAVIS, W. J. (1968a). The neuromuscular basis of lobster swimmeret beating. *J. exp. Zool.* **168**,
    363–78.
DAVIS, W. J. (1968b). Quantitative analysis of swimmeret beating in the lobster. *J. exp. Biol.* **48**,
    643–62,
DAVIS, W. J. (1969). The neural control of swimmeret beating in the lobster. *J. exp. Biol.* **50**, 99–117.
HARMON, L. D. & LEWIS, E. R. (1966). Neural modeling. *Physiol. Rev.* **46**, 513–91.
WILSON, D. M. (1964). Relative refractoriness and patterned discharge of locust flight motor neurons.
    J. exp. Biol. **41**, 191–205.